PORTLAND PRESS

Research Article

Comparative assessment of the bactericidal effect of nanoparticles of copper oxide, silver, and chitosan-silver against *Escherichia coli* infection in broilers

Eman I. Hassanen[1], Eman A. Morsy[2], Ahmed M. Hussien[3], Khaled Y. Farroh[4] and Merhan E. Ali[1]

[1]Pathology Department, Faculty of Veterinary Medicine, Cairo University, Giza 12613, Cairo, Egypt; [2]Poultry Disease Department, Faculty of Veterinary Medicine, Cairo University, Giza 12613, Cairo, Egypt; [3]Toxicology and Forensic Medicine Department, Faculty of Veterinary Medicine, Cairo University, Giza 12613, Cairo, Egypt; [4]Nanotechnology Department, Agricultural Research Center, Giza 12619, Cairo, Egypt

Correspondence: Eman I. Hassanen (eme_amr@hotmail.com, eme_amr@cu.edu.eg)

OPEN ACCESS

Escherichia coli infection is considered one of the most economically important multi-systemic diseases in poultry farms. Several nanoparticles such as silver, chitosan, and copper oxide are known to be highly toxic to several microbes. However, there are no data concerning their success against *in vivo* experimental *E. coli* infection in broilers. Therefore, the present study was designed to investigate the bactericidal effect of low doses of CuO-NPs (5 mg/kg bwt), Ag-NPs (0.5 mg/kg bwt), and Ch-Ag NPs (0.5 mg/kg bwt) against *E. coli* experimental infection in broilers. One hundred chicks were divided into five groups as follows: (1) control; (2) *E. coli* (4×10^8 CFU/ml) challenged; (3) *E. coli* +CuO-NPs; (4) *E. coli* +Ag-NPs; (5) *E. coli* +Ch-Ag NPs. The challenged untreated group, not NPs treated groups, recorded the lowest weight gain as well as the highest bacterial count and lesion score in all examined organs. The highest liver content of silver was observed in Ag-NPs treated group compared with the Ch-Ag NPs treated group. Our results concluded that Ch-Ag NPs not only had the best antibacterial effects but also acted as a growth promoter in broilers without leaving any residues in edible organs. We recommend using Ch-Ag NPs in broiler farms instead of antibiotics or probiotics.

Introduction

Poultry industry is primarily threatened by numerous microorganisms, which diminish the growth rate and cause broadly financial misfortunes. Among these, *Escherichia coli* is related to different manifestations in broilers and viewed as a significant foodborne pathogen in humans [1]. *E. coli* infection mostly occurs in chickens by using contaminated food, cross-contamination in breeding houses, or through slaughter and handling [2]. Consequently, more accentuation is probably centered on diminishing *E. coli* and other pathogens on poultry farms to reduce contamination with pathogens in prepared meats [3]. To increase livestock productivity, it is important to make diagnosis, treatment, and prevention of diseases. Currently, immunization and numerous antibiotics are used to combat microorganisms, but careless usage of antibiotics may cause wellbeing dangers to consumers [4]. Thus, it is interesting to examine other modern sorts of secure and successful biocidal compounds to battle poultry bacterial infections. Recently, nanotechnology has developed a modern promising innovation for nanoparticle synthesis in the nanometer size, which displays antimicrobial impacts related to their high surface area-to-volume proportion [5]. The antibacterial potentials of different metal and metal oxide nanoparticles such as copper, titanium, zinc,

and silver have been well reported [6]. Silver nanoparticles (Ag-NPs) are considered successful antibacterial agents against several microbes such as *E. coli*, *Vibrio cholera*, *Salmonella typhi*, and *Pseudomonas aeruginosa* [7,8]. Wide utilization of elemental silver or silver compounds in medical applications is due to the great antimicrobial efficiency of ionic silver (Ag^+) against various Gram-positive and -negative bacteria as well as fungi in combination of low toxicity against human tissue [9]. Thus, Ag-NPs may be a great candidate as an alternative for the formulation of a modern generation of antibacterial agents used in biological, medical, and pharmaceutical applications [10]. Ag-NPs can create their antibacterial action by disrupting the cell wall and cytoplasm, changing ATP levels, altering permeability and cell membrane respiration, hindering bacterial DNA replication, and creating free radicals, such as reactive oxygen species (ROS) [11]. The toxic effects of Ag-NPs still obscure and *in vivo* information of Ag-NPs toxicities are limited and disputable [12]. A few researchers have found that diverse surface stabilizers have imperative effects on Ag-NPs cytotoxicity. Chitosan is used as an active component of topical wound materials due to its great biocompatibility and antibacterial properties [13]. Numerous investigations have found that chitosan has been considered a good stabilizer for Ag-NPs and its antimicrobial efficacy [14]. In addition, chitosan-coated Ag-NPs showed great efficiency in killing common Gram-positive and -negative microbes, and fungi [15]. Copper oxide nanoparticles have been used in packaging and coatings of food because of their antimicrobial and antifungal properties. Like Ag-NPs, CuO-NPs have a wide spectrum of antibacterial effects against both Gram-positive and -negative microbes [16]. On account of the normal medicines by antibiotics lead to lack of biodiversity, the most punctual utilization of nanoparticles as an antimicrobial agent for treating different microbial infections is being developed [17]. In any case, *in vivo* studies related to the use of nanoparticles against poultry pathogens are excessively limited. Thus, the current study has made an endeavor to discover novel antibacterial agents from metal and metal oxide nanoparticles for treating *E. coli* infections in broiler chickens. The NPs were selected due to their significance in food safety applications.

Materials and methods
Bacterial strain isolation, identification, and counting
E. coli isolate O_{78} was previously isolated from broiler chicks suffered from high mortalities, serotyped and detected for its virulence via Congo Red binding assay [18]. *E. coli* O_{78} serotype was grown aerobically in nutrient broth at $37°C$ for 24 h before using as a target organism. The dose was calculated to match 4×10^8 CFU/ml of bacterial isolate.

Preparation of copper oxide nanoparticles
Copper oxide nanoparticles were prepared by chemical precipitation method according to the method described by **Hassanen et al.** [19].

Preparation of Ag-NPs
Ag-NPs colloidal solution (17 ± 5 nm) was prepared by co-precipitation protocol through the reduction of silver nitrate ($AgNO_3$) (99.99%, Aldrich, U.S.A.) with sodium borohydride (99%, Aldrich, U.S.A.) under boiling conditions [20]. The concentration of silver in the prepared solution was 10 mM.

Preparation of chitosan-AgNPs
Chitosan-silver nanocomposites (Ch-Ag NCs) were prepared by reduction of silver nitrate by chitosan according to the method described by **Hassanen et al.** [21]. The concentration of silver in the prepared solution was 10 mM.

Characterization of the prepared nanoparticles
Actual morphology and size of nanoparticles were assessed by High Resolution Transmission Electron Microscope (HR-TEM) operating at an accelerating voltage of 200 kV (Tecnai G2, FEI, Netherlands). Dynamic light scattering (DLS) technique was utilized to estimate the average particle size distribution that was measured by zeta sizer (Malvern, ZS Nano, U.K.). The chemical structure of the prepared nanoparticles was assessed using X-ray diffraction (XRD) technique.

Acute toxicity study to determine LD$_{50}$ of the selected nanoparticles
A total of 60 commercial broiler (Cobb 500) chicks (7-day-old) were used to determine LD_{50} of Ag-NPs, Ch-Ag NPs, and CuO-NPs. They were divided into different groups according to different doses of the treated nanoparticles. The LD_{50} value was calculated according to **Weil** [22] as in the following equation:

$$\mathbf{Log\ LD_{50} = Log\ D_a + d\ (f + 1).}$$

Log Da $=$ log of the lowest of the four dosage levels used, **d** $=$ logarithm of geometric factor (R), **f** $=$ R-values in the table.

Animals and experimental design

All the procedures of the experiment were done according to the guidelines of the Institutional Animal Care and Use Committee at Cairo University and approved by Vet-CU-IACUC (approval number: 0722019057), Cairo, Egypt.

A total of 100 one-day-old mix (Cobb 500) broiler chicks were obtained from El-Hawamdya-Giza. The birds were resided in pens on straw litter and reared in standard hygiene conditions in a building with regulated temperature and humidity. The birds had permanent access to drinking water and received *ad libitum* complete feed mixtures appropriate for the rearing period according to the nutrient requirements of broilers.

The chicks were randomly divided into five groups of 20 birds each. Group (1) was kept as a control group and received normal saline daily by oral gavage for 7 days (control negative). Group (2) was challenged at 7th day of age by crop gavages with 4×10^8 CFU/ml/bird of *E. coli* serogroup O_{78} in PBS for 2 successive days according to the method described by **Awaad et al.** [23] and left untreated; group (3) was challenged and treated by 5 mg/kg bwt CuO-NPs daily by oral gavage for 7 days; group (4) was challenged and treated by 0.5 mg/kg bwt Ag-NPs daily by oral gavage for 7 days; group (5) was challenged and treated by 0.5 mg/kg bwt Ch-Ag NPs daily by oral gavage for 7 days. The dose of different nanoparticles is obtained from the acute toxicity study which represented 1/20 LD_{50}. All birds were monitored and weighted weekly all over the experimental period.

Sampling

At 21 days, all birds were admitted to PM room to collect blood and organ samples. Blood samples were collected aseptically from wing vein and used freshly for bacterial count. All birds were slaughtered by exsanguination without using anesthesia to collect liver, spleen, intestine, kidneys, heart, and bursa of Fabricius. Some of these organs preserved at $-80°$C till used for bacterial re-isolation, while others preserved in 10% neutral buffered formalin for histopathological examinations.

Bacterial re-isolation

The blood and organ (liver and spleen) tissue homogenates were then ten-fold serially diluted before platting on EMB agar for plate counting. Biochemical identification was performed using API 20-Etest kit (bioMérieux Inc., Marcy l'Etoile, France) according to the manufacturer's instructions [24]. Serological identification of the isolated *E. coli* was done using *E. coli* antisera (Denka Seiken, Japan) according to the method described by **Blanco et al.** [25].

Histopathological examinations

Formalin-fixed tissue specimens were processed via conventional methods and sliced into 4 mm sections to obtain paraffin-embedded tissue sections stained by H&E to be examined under light microscope for histopathological examination [26].

Microscopic grading and scoring were performed to document lesion severity of the examined organs in different treated groups. The grading criteria for degenerative, necrotizing, and inflammatory lesions were assessed as none, slight, mild, moderate, and severe as follow; 0 (normal histology), 1 (<25%), 2 (25:50%), 3 (50:75%), 4 (>75% tissue damage) according to method described by **Hassanen et al.** [27]. While grading scheme for multifocal lesions assessed according to the method documented by **Hassanen et al.** [28] as follow: (0) no foci; (1) <3 foci; (2) 3–6 foci; (3) 7–12 foci; (4) >12 foci.

Nanoparticle content in different organs

Flame atomic absorption spectrophotometer (ZEISS, AAS5, and Germany) was used to measure the contents of copper and silver in muscle and some edible organs such as heart, liver, and spleen tissue homogenate [19]. Briefly, concentrated nitric acid and 30% H_2O_2 were added to 0.5 g tissue samples and kept overnight, then heated in a microwave digestion system (ETHOS One; Milestone, Sorisole, Italy) till it became completely digested and colorless. Afterward, the samples were allowed to cool, and the remaining solutions were diluted with 2% nitric acid.
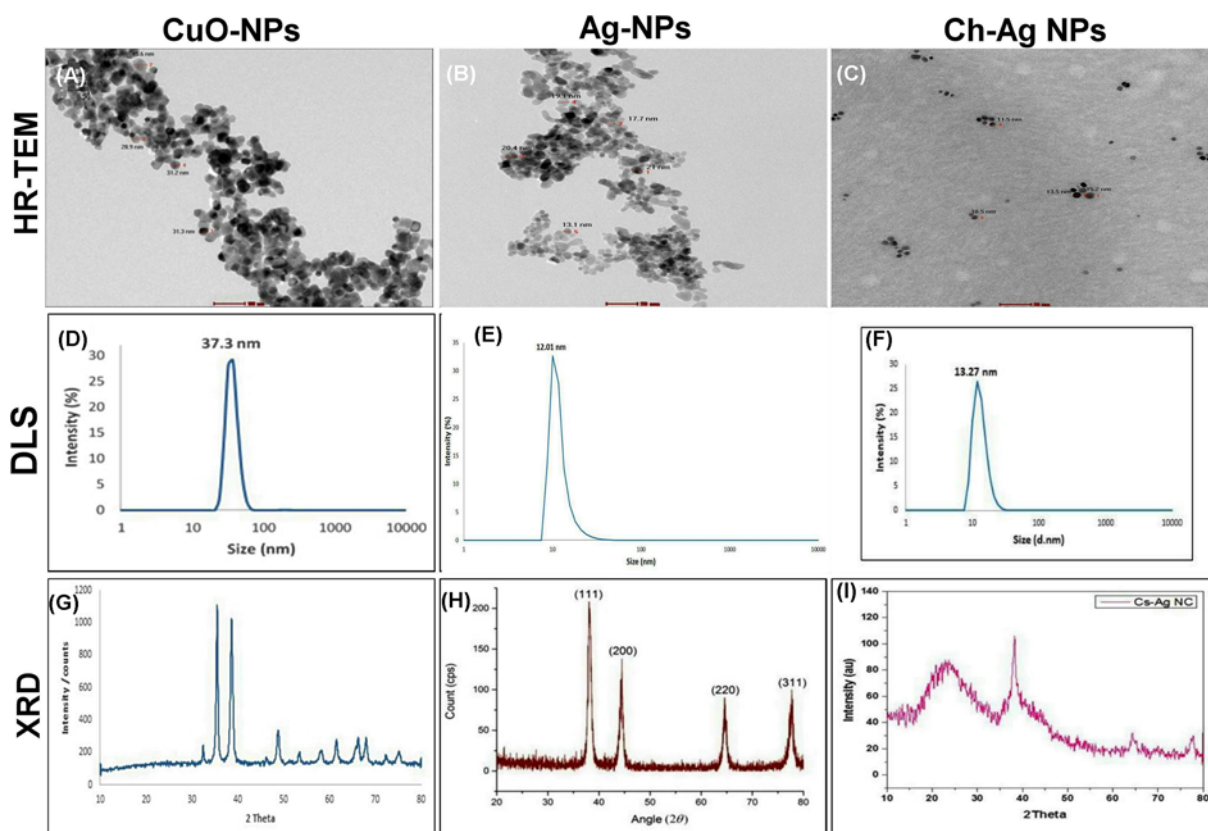
Figure 1. Characterization of the prepared nanoparticles

(**A–C**) High resolution-transmission electron microscopic image of different NPs. (**D–F**) Particle size distribution curve obtained from DLS measurements. (**G–I**) XRD pattern of NPs.

Statistical analysis

Statistical analysis was performed utilizing SPSS version 16.0 software (SPSS Inc., Chicago, IL, U.S.A.). Values were expressed as means $\pm$ SEM. Comparison of means between several groups was performed by one-way analysis of variance (ANOVA) and independent t test was used to compare between two groups. Values were considered statistically significant at $P \leq 0.05$.

Results

Characterization of nanoparticles

HR-TEM images showed spherical-shaped CuO-NPs with average size $\sim$28.9–45.6 nm (Figure 1A). Ag-NPs showed well uniformed spheres with average size of 17 ± 5 nm (Figure 1B). Ch-Ag NCs showed spherical shaped nanoparticles with average particle size 17.5 nm distributed homogeneously in the Ch matrix (Figure 1C). The particle size distribution curve obtained from DLS measurements were 37.3, 17.3, 20 nm for CuO-NPs, Ag-NPs, and Ch-Ag NCs, respectively (Figure 1D–F). XRD pattern of CuO-NPs showed peaks at $2\theta = 32.48°$, $35.54°$, $38.64°$, $48.85°$, $61.52°$, 65.66, 66.34, and $68.02°$ were assigned to (110), ($-$111), (111), ($-$202), ($-$113), (022), ($-$311), and (220) of CuO nanoparticles, indicating that the crystalline structure of synthesized Cu nanoparticles presented a hexagonal wurtzite structure (Zincite, JCPDS 04-005-4712) (Figure 1G). XRD pattern of Ag-NPs showed sharp intense and narrow peaks at $38.14°$, $44.41°$, $64.61°$, and $77.74°$ 2θ angles those corresponding to *hkl* parameters of (111), (200), (220), and (311), respectively (Figure 1H). The obtained diffraction pattern was compared with the standard ICCD library installed in PDF4 software, card no: (04-003-5625). XRD pattern of Ch-Ag NCs showed a peak of chitosan at 2θ value of the broad peak $\sim$15–35°. The peaks of silver were indexed to the face-centered cubic structure which is in good agreement to the JCPDS card No. 04-004-8730. The three silver peaks obtained belong to the (111), (220), and (311) reflections, respectively. The results showed that the synthesized nanoparticles were Ag-NPs because the position and relative intensity of all the diffraction peaks of the samples were consistent with the crystalline pattern of

Table 1 Mortality data in 7-day-old chicks received single oral doses of different nanoparticles in different groups

Groups	1	2	3	4
CuO-NPs				
Dose (mg/kg)	27	40.5	60.75	91.125
Number of birds/group	5	5	5	5
Number of dead birds/group	0	1	2	5
Ag-NPs				
Dose (mg/kg)	3.1	6.2	12.4	24.8
Number of birds/group	5	5	5	5
Number of dead birds/group	0	1	3	5
Ch-Ag NPs				
Dose (mg/kg)	120	240	480	960
Number of birds/group	5	5	5	5
Number of dead birds/group	0	2	2	5
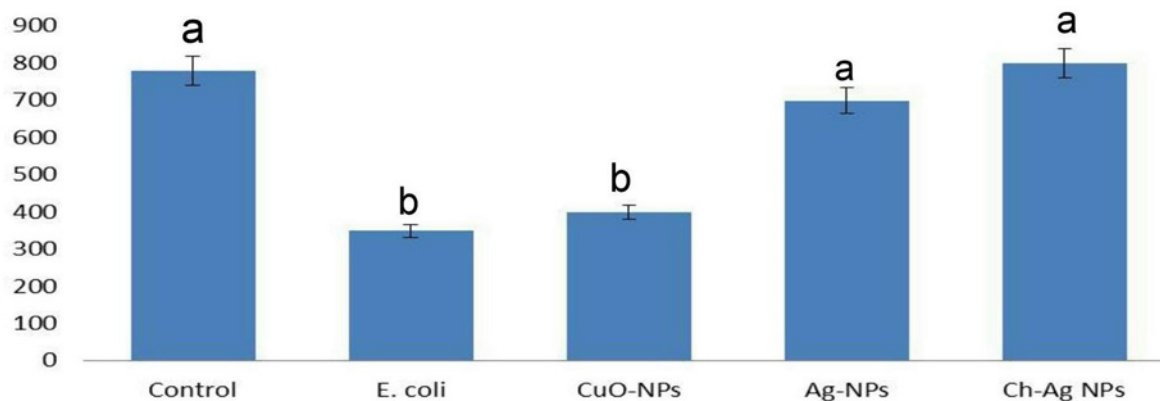
Figure 2. The effect of different treatments on mean body weights of birds
Bar charts representing mean body weights of birds in different groups. Values were presented as mean $\pm$ SEM ($n = 20$ birds/group). Values with different letters (a,b) are considered significantly different at $P \leq 0.05$.

silver. The presence of chitosan, silver, and the absence of impurity phases were evident from the XRD image (Figure 1I).

Acute toxicity study of the prepared nanoparticles

Mortalities recorded within 24 h after oral administration of CuO-NPs, Ag-NPs, and Ch-Ag NPs in different treatment groups were recorded in (Table 1). The calculated oral LD_{50} of CuO-NPs, Ag-NPs and Ch-Ag NPs in 7-day-old chicks (Cobb 500) equals 100, 10, 381 mg/kg bwt for each nanoparticle, respectively.

The effect of different treatments on the body weight and mortality of birds

The results summarized in Figure 2 showed remarkable reduction in mean body weight of broiler chickens in challenged untreated group. There was a noticeable increasing in body weights of chickens in group treated with Ch-Ag NCs compared with control group. On the other hand, there was no significant difference in mean body weight of birds in nanoparticles treated groups compared with control group. The highest mortality rate was recorded in the challenged untreated group (40%) followed by CuO-NPs treated group (20%). On the other side, no mortality recorded in both control group and those treated with either Ag-NPs or Ch-Ag NPs.

Table 2 The effect of different treatments on the mean *E. coli* count (CFU/ml) in the blood and different organs after 21 days post challenge

	Blood	Liver	Spleen
Control	0 ± 0^A	0 ± 0^A	0 ± 0^A
E. coli	180 ± 42^B	219 ± 54^B	197 ± 46^B
CuO-NPs	$115 \pm 12^{B,b}$	$150 \pm 56^{B,b}$	$130 \pm 22^{B,b}$
Ag-NPs	$35 \pm 5^{C,c}$	$44 \pm 7.5^{C,c}$	$40 \pm 2.2^{C,c}$
Ch-Ag NPs	$9 \pm 1.1^{C,a}$	$8.5 \pm 2^{C,a}$	$9.8 \pm 1.2^{C,a}$

Value was demonstrated as mean $\pm$ SEM. Value with different letters considered significantly different at $P \leq 0.05$ (*n*=7 birds/group). Capital letters indicate significance between all five groups while small letters indicate significance between the three nanoparticles treated groups.

Table 3 Copper contents in different organs of CuO-NPs treated or untreated groups

	Control	CuO-NPs
Muscle	1.7 ± 0.02^a	2.2 ± 0.07^b
Liver	2.5 ± 0.12^a	2.6 ± 0.32^a
Spleen	2.5 ± 0.23^a	2.6 ± 0.13^a
Heart	1.5 ± 0.21^a	2.2 ± 0.11^b

Values were presented as mean $\pm$ SEM (*n*=7 birds/group). Values with different letters considered significantly different at $P \leq 0.05$.

Table 4 Silver contents in different organs

	Control	Ag-NPs	Ch-Ag NPs
Muscle	0 ± 0^A	0.001 ± 0^{Aa}	$0 \pm 0^{A,a}$
Liver	0 ± 0^A	$31.3 \pm 1.24^{B,b}$	$3.4 \pm 0.26^{A,c}$
Spleen	0 ± 0^A	$4.2 \pm 0.9^{B,b}$	$0.001 \pm 0^{A,c}$
Heart	0 ± 0^A	$0.002 \pm 0^{A,a}$	$0 \pm 0^{A,a}$

Values were presented as mean $\pm$ SEM (*n*=7 birds/ group). Values with different letters considered significantly different at $P \leq 0.05$. Capital letters A and B indicate significance between all groups while small letters a, b, and c indicate significance between nanoparticles treated groups.

Bacterial re-isolation

There was a remarkable reduction in the *E. coli* count in groups treated either with Ag-NPs or Ch-Ag NPs (∼80, 95%, respectively) in blood and different organs (liver and spleen) compared with challenged untreated group. Approx. 50% reduction in the *E. coli* count observed in both blood and organs obtained from CuO-NPs treated group compared with the challenged untreated group (Table 2).

Nanoparticles contents in muscle and edible organs

There was a significant increase in copper contents in muscle, spleen, and heart in CuO-NPs treated group compared with the control group (Table 3). Whereas, a significant increase in silver contents of liver of birds in Ag-NPs treated group were reported. On the other hand, there were no significant difference in silver content in muscle, spleen, and heart in the groups treated with either Ag-NPs or Ch-Ag NPs compared with the control group (Table 4).

Histopathological examinations

Microscopic pictures in all examined organs obtained from the control negative group showed normal histological structures. On the other hand, the *E. coli* challenged group showed severe to moderate pathological alterations in all examined organs with remarkable improvements in all the treated groups.

Small intestine of the challenged group showed extensive acute enteritis with destruction of intestinal villi (Figure 3A). There were extensive degenerations and necrosis in the epithelial lining intestinal mucosa associated with remarkable hyperplasia of the goblet cell (Figure 3B). Fibrinous exudates, necrotic cell debris, and inflammatory cells were collected and forming pseudo-membrane covering the intestinal mucosa. Lamina propria and submucosa severely infiltrated with heterophils and mononuclear inflammatory cells (Figure 3C). Remarkable improvements were recorded in all the treated groups, but the best microscopic picture observed in groups treated with Ch-Ag NPs.
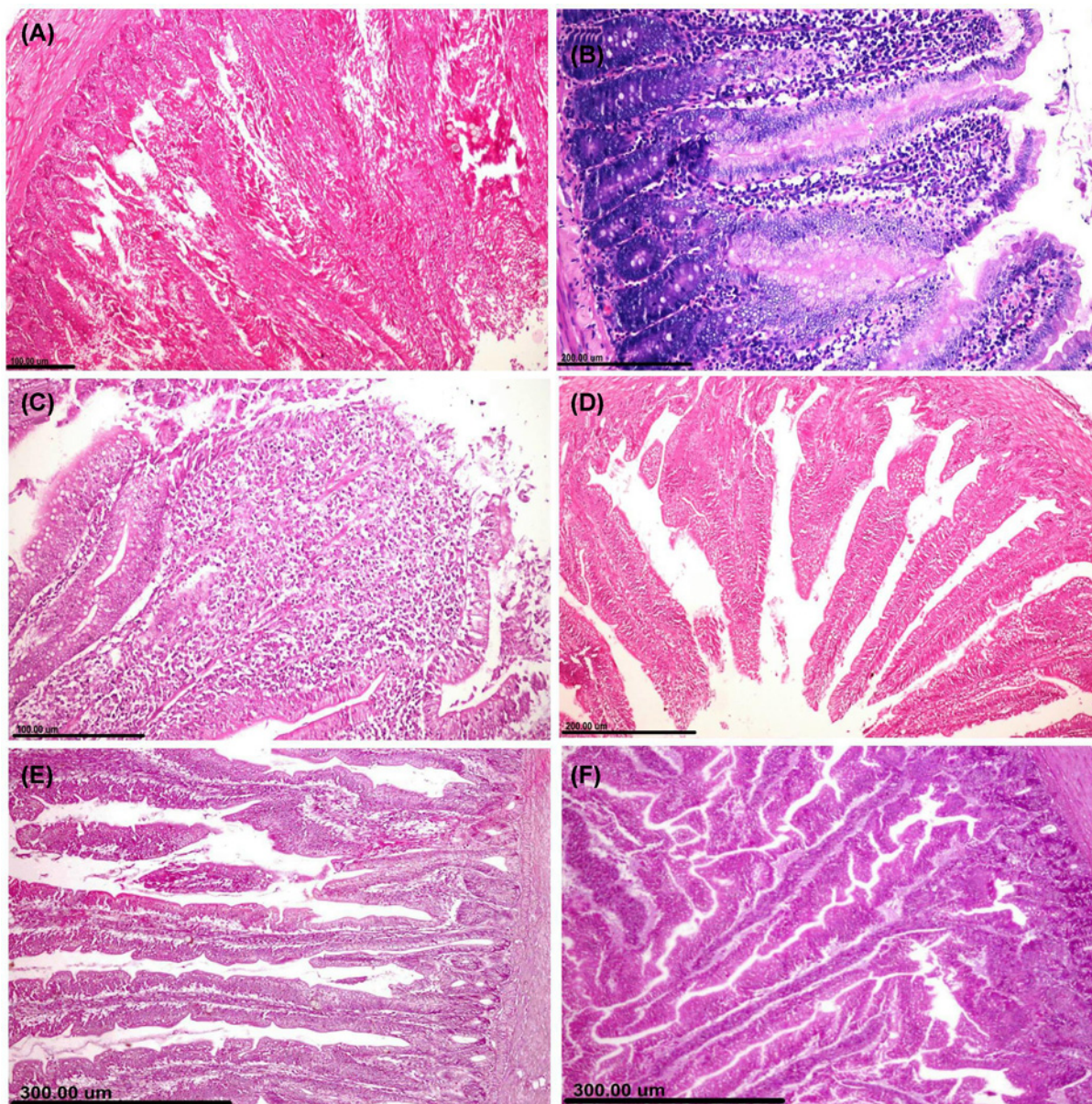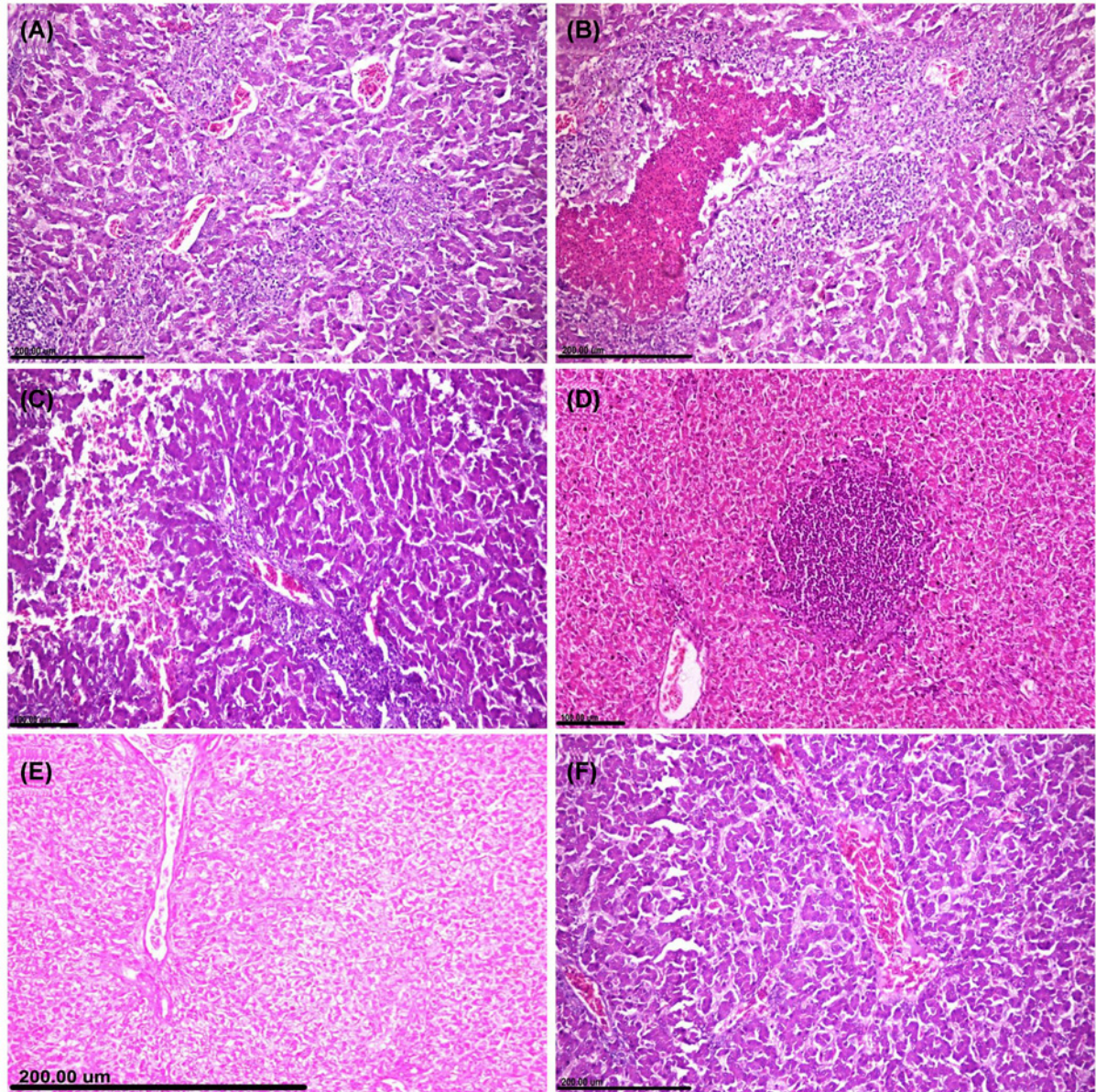
Figure 3. The effect of different treatments on the histopathological pictures of the intestine

Photomicrographs of intestinal tissue sections stained with H&E representing, (**A–C**) *E. coli* challenged untreated group showing. (A) Complete destruction of the intestinal villi with fibrinous adhesion. (B) Necrosis of intestinal epithelium with extensive hyperplasia of goblet cells. (C) Extensive widening of lamina propria with inflammatory cells and exudates. (**D**) CuO-NPs treated group showing shortening of intestinal villi with reduction of crypt depth. (**E**) Ag-NPs treated group showing increasing in both height of intestinal villi and crypt depth with minimum inflammatory reactions. (**F**) Ch-Ag NPs treated group showing remarkable increasing in the intestinal villi and crypt depth.

Otherwise, the group treated with CuO-NPs showed degeneration and necrosis in some of the epithelial lining intestinal mucosa associated with mild to moderate inflammatory cells infiltration in lamina propria and submucosa (Figure 3D). In spite of extensive hyperplasia of goblet cells and mild inflammatory reactions observed within the intestinal mucosal layers of AgNP-treated group (Figure 3E), Ch-Ag NPs treated group showed normal histological structures (Figure 3F).

Liver of the challenged group showed extensive hepatocellular degeneration and necrosis. Multifocal areas of hepatocellular coagulative necrosis were detected and infiltrated with inflammatory cells replacing the hepatic parenchyma

Figure 4. The effect of different treatments on the histopathological pictures of the liver
Photomicrographs of hepatic tissue sections stained with H&E representing, (**A–C**) *E. coli* challenged untreated group showing. (A) Coalescent areas of hepatocellular coagulative necrosis infiltrated with mononuclear inflammatory cells. (B) Portal tried showing severe congestion and inflammatory cells infiltrations. (C) Focal hemorrhage. (**D**) CuO-NPs treated group showing focal coagulative necrosis infiltrated with inflammatory cells. (**E**) Ag-NPs treated group showing diffuse hepatocellular cytoplasmic vacuolization. (**F**) Ch-Ag NPs treated group showing normal histological structures.

(Figure 4A). Cholangiohepatitis noticed in some cases and characterized by portal edema and inflammatory cells in-filtration (Figure 4B). There was hyperplasia in the epithelial lining bile duct associated with the presence of newly formed bile ductules. Perihepatitis observed in most sections manifested by extensive widening of the hepatic cap-sule by fibrinous exudates and inflammatory cells infiltrations. Multifocal to coalescent areas of hemorrhage were noticed within the hepatic parenchyma (Figure 4C). Group treated with CuO-NPs showed focal area of hepatocellu-lar necrosis infiltrated with inflammatory cells (Figure 4D). Group treated with Ag-NPs showed moderate to diffuse hepatocellular cytoplasmic vacuolization (Figure 4E). Remarkable improvements were recorded in the group treated with Ch-Ag NPs and the liver sections appeared with normal histological structures (Figure 4F).

Heart of the challenged group showed moderate fibrinous pericarditis characterized by congestion of blood vessels, thickening in the pericardium by fibrinous exudates and inflammatory cell infiltrations (Figure 5A). Cardiac muscle noticed severe degeneration and necrosis associated with congestion and inflammatory cell infiltration. CuO-NPs treated group showed mild to moderate degeneration and necrosis in the cardiac muscle (Figure 5B). On the other side, groups treated with either Ag-NPs (Figure 5C) or Ch-Ag NPs (Figure 5D) showed remarkable improvements and the organ appeared with normal histological structures.

Kidneys of the challenged group showed interstitial tubule-nephritis characterized by interstitial congestion, hemorrhage, edema, and inflammatory cells infiltration (Figure 5E). Renal tubular epithelial cells suffered from several degenerative changes and necrosis with intracellular and intraluminal hyaline cast and droplets. Kidneys of the group treated with CuO-NPs showed moderate degeneration and necrosis in the epithelial lining renal tubules associated with interstitial inflammatory reactions (Figure 5F). Ag-NPs treated group showed several degenerative changes in the tubular epithelium with interstitial hemorrhage (Figure 5G). Remarkable improvements observed in the group treated with Ch-Ag NPs (Figure 5H) compared with other nanoparticles-treated group and the kidneys appeared with normal histological structures.

Spleen of the challenged group showed mild to moderate pathological alterations manifested by lymphocytic cell depletion in some lymphoid follicles (Figure 6A). On the other hand, spleen tissue sections in nanoparticle-treated groups showed normal histological structures (Figure 6B–D).

Bursa of Fabricius of the challenged group showed extensive lymphocytic cell depletion in most lymphoid follicles associated with marked thickening in the inter follicular septa by edema and inflammatory cell infiltrations (Figure 6E). Group treated with CuO-NPs showed moderate lymphocytolysis with prominent follicular septa between cortex and medulla (Figure 6F). In spite of moderate lymphocytolysis occurred in some lymphoid follicles of Ag-NPs treated group (Figure 6G), bursa obtained from Ch-Ag NPs treated group showed normal histological structures (Figure 6H).

Lesion scoring in all examined organs of different treated groups was illustrated in (Figure 7). The highest score noticed in the *E. coli* challenged group, while the lowest score noticed in the group treated with Ch-Ag NPs. Reduction in lesion scoring observed in an ascending order for CuO-NPs and Ag-NPs.

Discussion

The expansion of bacterial strains showing resistance from different antimicrobials has encouraged researchers just as the food business administrators to search for other antimicrobial options. Nanotechnology may introduce a probable solution for this problem and there are different kinds of nanoparticles usually viewed as a wide-range antimicrobial specialist especially metal oxide and Ag-NPs [29,30]. The antibacterial potentials of NPs are poorly understood in broiler chickens; therefore, our study was designed to investigate and compare between the possible antibacterial effect of nanoparticles of CuO, Ag, and Ch-Ag against *E. coli* experimental infections in broiler chickens.

In the present study, *E. coli* challenged, and untreated groups showed extensive reduction in body weight and this is consistent with **Rosa et al.,** who attributed the decreased weight gain to the oxidative stress caused by *E. coli* [31]. These results reflected on the pathological pictures and bacterial re-isolation in different organs of this group, which showed the highest lesion score and bacterial count in all examined organs. Our histopathological results were come in accordance with **Sawah et al.,** who observed fibrinonecrotic enteritis, fibrinous perihepatitis, and fibrinous pericarditis in chickens infected with *E. coli* [32]. Another recent study reported that *E. coli* infection resulted in depletion of lymphocytes in bursa and spleen [33].

The present study showed an increase in the bactericidal effect in an ascending order for CuO-NPs, Ag-NPs, and Ch-Ag NPs. Although the CuO-NPs exert moderate antibacterial effects against *E. coli* experimental infection in broiler chickens, it is considered to be toxic to the broilers and elicit pathological alterations in all examined organs. Flame atomic absorption spectroscopic results observed an increase in the copper content in muscle and other edible organs, suggesting that the microscopic lesions observed in the CuO-NPs treated group is related to the CuO-NPs itself not to *E. coli* infections. Indeed, CuO-NPs reduced ∼50% of the bacterial count in the liver, spleen, and heart compared with the challenged untreated group. Our findings were some extent similar to **Al-Jassani and Raheem**, who found that CuO-NPs have considerable powerful inhibitory and anti-bacterial effect on *E. coli* [34]. Several studies have investigated the in vitro antimicrobial effects of CuO-NPs on different kinds of food-borne pathogens as *Staphylococcus aureus*, *E. coli*, and *Klebsiella pneumonia* [35]. The antibacterial activity of CuO-NPs could be attributed to the sudden decline in bacterial cell membrane integrity in addition to the release of ROS, which contribute to the degradation of several biomolecules that affect also on normal cell viability [36,37].

Rather than CuO-NPs treated group, other NP-treated groups showed marked improvements in body weights and the best results were observed in the group treated with Ch-Ag NPs. Our findings may be related to the biological
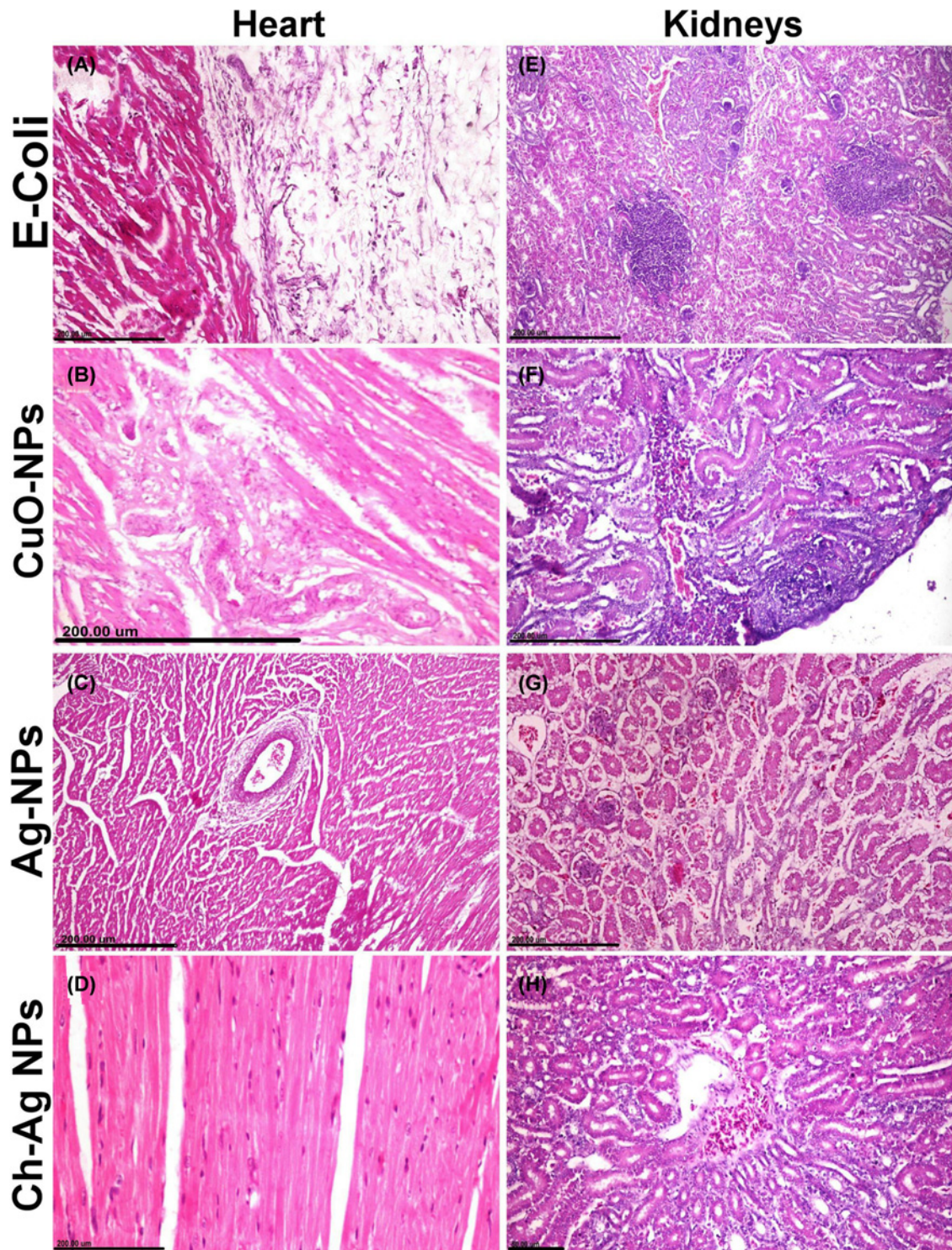
Figure 5. The effect of different treatments on the histopathological pictures of the heart and kidney tissues
(**A–D**) Photomicrographs of cardiac tissue sections stained with H&E representing, (A) *E. coli* challenged untreated group showing fibrinous pericarditis. (B) CuO-NPs treated group showing coagulative necrosis and vacuolar degeneration of cardiac muscle. (C,D) Groups treated with Ag-NPs and Ch-Ag NPs respectively showing normal histological structures. (**E–H**) Photomicrographs of kidney sections stained with H&E representing, (E) *E. coli* challenged untreated group showing focal interstitial nephritis. (F) CuO-NPs treated group showing moderate tubulointerstitial nephrotoxic nephritis. (G) Ag-NPs treated group showing marked interstitial edema and hemorrhage with minimum inflammatory cells infiltrations. (H) Ch-Ag NPs treated group showing normal histological structures.
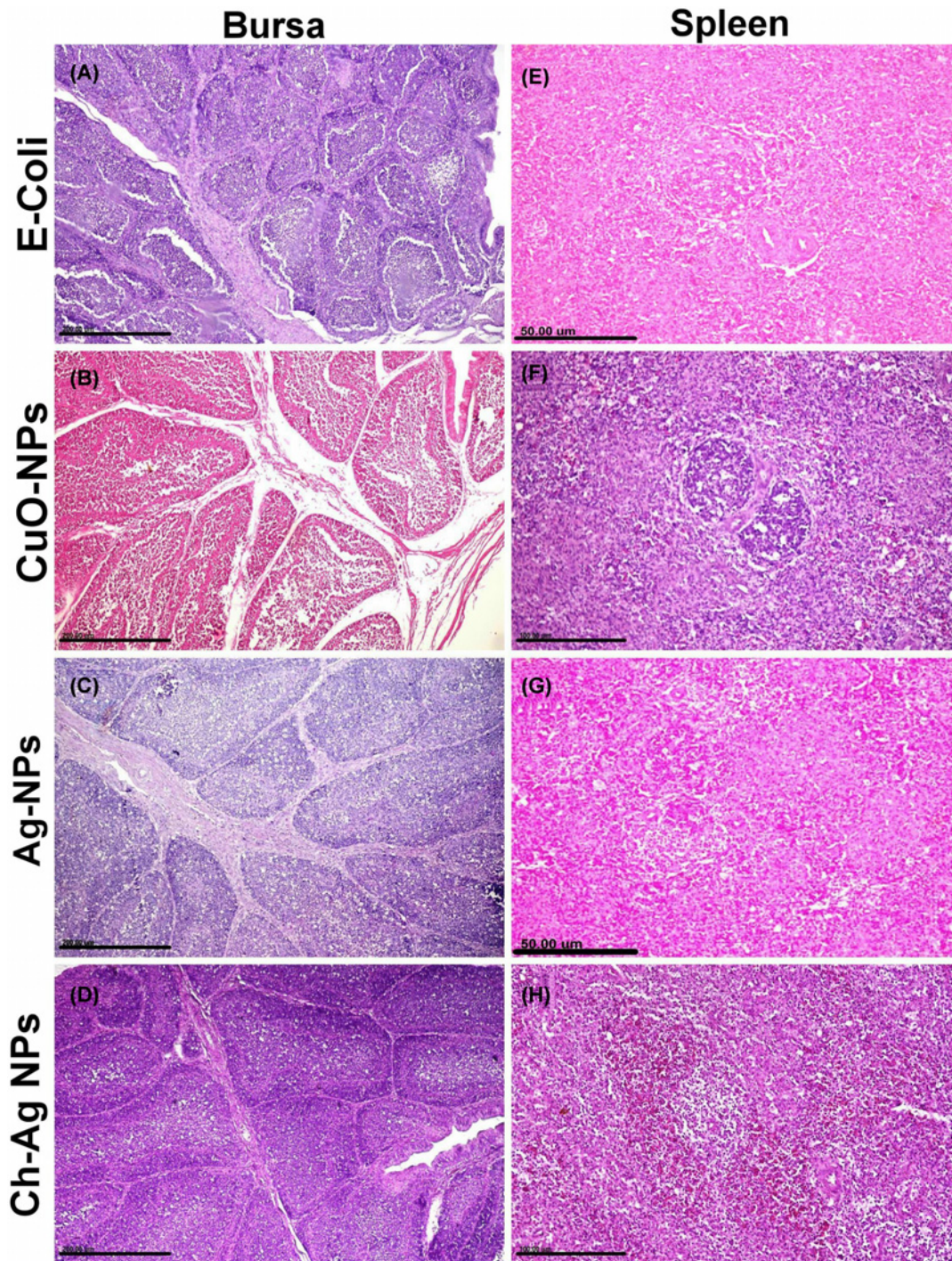
Figure 6. The effect of different treatments on the histopathological pictures of bursa of Fabricius and spleen

(**A–D**) Photomicrographs of bursa tissue sections stained with H&E representing, (A) *E. coli* challenged untreated group showing widening of interfollicular septa by fibrinous exudates and inflammatory cells with marked lymphocytic depletion. (B) CuO-NPs treated group showing moderate lymphocytolysis with prominent basement membrane between follicular cortex and medulla. (C) Ag-NPs treated group showing extensive lymphocytolysis with interfollicular fibrosis and inflammatory cells infiltrations. (D) Ch-Ag NPs treated group showing normal histological structures. (**E–H**) Photomicrographs of spleen tissue sections stained with H&E representing, (E) *E. coli* challenged untreated group showing mild lymphocytic cell depletion in periarteriolar lymphoid follicles of splenic white pulp. (F) CuO-NPs treated group showing extensive lymphoid cell depletion in lymphoid follicles with huge number of tangible body macrophages. (G,H) Groups treated with Ag-NPs and Ch-Ag NPs, respectively, and showing normal histological structures.
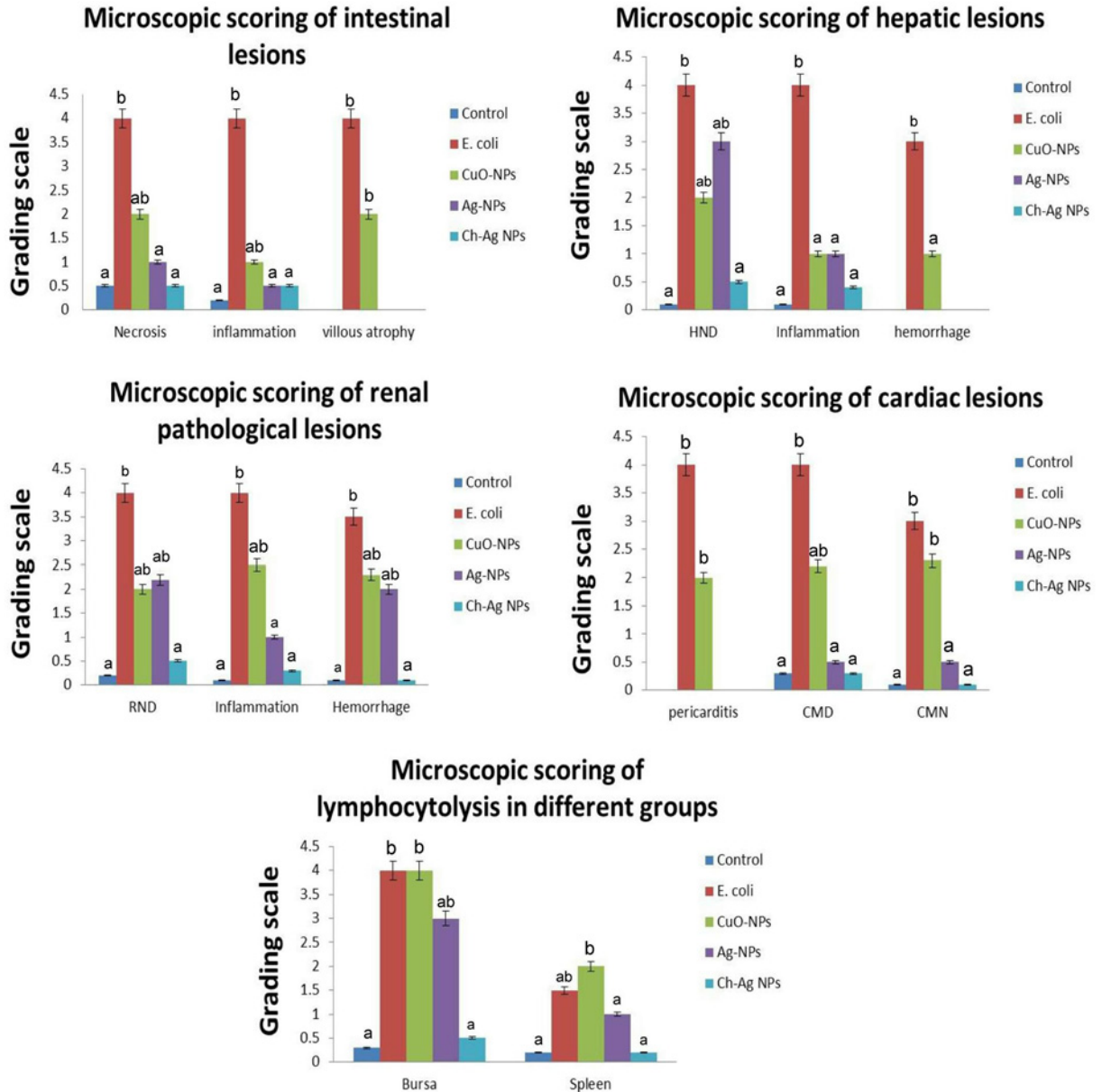
Figure 7. Bar charts representing microscopic lesion scoring in different organs of different treated groups
Values were presented as mean $\pm$ SEM (*n*=7 birds/ group). Values with different letters considered significantly different at $P \leq 0.05$.
Abbreviations: CMD, cardiac muscle degeneration; CMN, cardiac muscle necrosis; HND, hepatocellular necrosis and degeneration; RND, renal tubular necrosis and degeneration.

effects of both silver and chitosan on intestinal harmful bacteria, which resulted in improved growth as the absorption of nutrients was increased [38]. Additionally, NPs could increase intestinal absorption and utilization of minerals required for improving growth performance by increasing the surface area [39]. Our histopathological results showed an increase in the height of the intestinal villi and crypt depth in both Ag and Ch-Ag NPs treated groups, suggesting improved mineral and nutrient absorption in such groups. Similarly, as antibiotics, Ag-NPs are relied upon improving the well-being of animals. That is, Ag-NPs allowing them the chance to consume fewer supplements on the metabolic exertion required for immunological control and to use additional supplements for other physiological and gainful purposes [40].

PORTLAND
PRESS

The best antibacterial effect was noticed in Ch-Ag NPs treated group compared with other NPs treated groups, which manifested by a marked reduction in both bacterial count and lesion score in all examined organs. This is attributed to the potent antibacterial capacity of both silver and chitosan nanoparticles [41,42]. The bactericidal action of Ag-NPs might be because of a brief balance of the surface electric charge of the bacterial membrane promoting bacterial death [43–45]. Moreover, the generation of ROS restrains the antioxidant defense mechanism leading to further damage to the cell membrane. Chitosan is a nonpoisonous biopolymer obtained from shellfish and showed an amazing antibacterial activity [46]. **Du et al.** found that the antimicrobial properties of chitosan were improved extensively by loading it with different metals [47]. The bactericidal effects of NPs depend on their particular physicochemical properties [48,49]. Rather than traditional antibiotics, NPs have peculiar dimensions <100 nm. Their uniquely small size outcomes in novel properties, as more prominent interaction with cells because of a larger surface area-to-mass ratio and flexible and controllable application [50,51].

The current study revealed a significant increase in silver content of the liver of birds in the group treated with Ag-NPs in contrast with those treated with Ch-Ag NPs. Our findings suggest that the accumulation of Ag-NPs in the liver of broiler chickens may be transferred to consumers leading to several side effects. These results are in harmony with several previous studies showed a marked increase in Ag retention in the liver more than in muscular tissue and other organs in broiler chickens [52,53]. Chitosan nanoparticles contain unique functional groups (amino groups) that interact with silver ions, in addition, nanoparticles as well act as capping sites for nanoparticle stabilization [54]. Moreover, Ch-NPs not only act as matrix or capping agent but also act as stabilizing agent for Ag-NPs by forming a network on NP surface allows the homogeneous Ag-NPs distribution on the surface, with no visible aggregation effects [55]. This, in turn, determines the potential bactericidal effects of Ch-Ag NPs and their bioavailability by covering the external surface of the carrier [56]. We suggest that coating of silver NP core by chitosan can reduce particle aggregation and improve their solubility, bioavailability, and stability, so that, it prevents accumulation of silver in organs and increasing their excretion.

Conclusions

From our results, we concluded that Ch-Ag NPs had a powerful bactericidal activity against *E. coli*, which neither reduced body weight gains nor leaving toxic residues in muscles and edible organs. Alternatively, CuO-NPs not only reduced body weights of birds but also caused extensive pathological alterations in different organs associated with increasing copper levels in such organs. Our results find that chitosan nanoparticles not only have the ability to increase the antibacterial effect of Ag-NPs but also it can reduce their bioaggregation and toxicity in different organs. Therefore, we highly recommended using Ch-Ag NPs as an alternative antibacterial agent in treating infections without taking the risk of developing resistant bacterial strains as with antibiotics. In addition, further studies are required to discuss the mechanism of action of chitosan nanoparticles and how it can prevent the accumulation of silver or other NPs in body organs. Moreover, more studies are needed to compare the effect of metal nanoparticles and those coating with chitosan to confirm the ability of Ch-NPs either on detoxifying or improve the efficacy of many metallic and metal oxide nanoparticles.

Data Availability

All data will be available on request to the corresponding author.

Competing Interests

The authors declare that there are no competing interests associated with the manuscript.

Funding

Author Contribution

E.I.H. and E.A.M. conceived the study and designed the experiment as well as reviewed all the results, carried out data analysis and drafted the manuscript. E.I.H. and M.E.A. performed the pathological studies. E.A.M. performed the microbiological studies and carried out the experiment. A.M.H. performed the acute toxicity studies. K.Y.F. prepared and characterized the nanoparticles. All authors wrote, read, revised, and approved the final manuscript.

Ethics Approval

All the animal management and the experimental procedures for the current study were done in the Laboratory Animal Housing, Department of Toxicology and Forensic Medicine, Faculty of Veterinary Medicine, Cairo University and approved by Institutional Animal Care and Use Committee at Veterinary Medicine, Cairo University (Vet-CU-IACUC-approval number: 0722019057), Cairo, Egypt and conducted according to the guidelines of the laboratory animal care and use committee (8th edition 2011).

Abbreviations

Ag-NP, silver nanoparticle; bwt, body weight; Ch-AgNC, chitosan-silver nanocomposite; DLS, dynamic light scattering; H&E, hematoxylin and eosin; HR-TEM, High Resolution Transmission Electron Microscope; PM, postmortem examinations; ROS, reactive oxygen species; XRD, X-ray diffraction.

References

1 Bezerra, W.G.A., da Silva, I.N.G., Vasconcelos, R.H., Machado, D.N., de Souza Lopes, E., Lima, S.V.G. et al. (2016) Isolation and antimicrobial resistance of Escherichia coli and Salmonella enterica subsp. enterica (O: 6,8) in broiler chickens. *Acta Sci. Vet.* **44**, 1–7

2 Losasso, C., Belluco, S., Cibin, V., Zavagnin, P., Mičetić, I., Gallocchio, F. et al. (2014) Antibacterial activity of silver nanoparticles: sensitivity of different Salmonella serovars. *Front. Microbiol.* **5**, 227, https://doi.org/10.3389/fmicb.2014.00227

3 EFSA and ECDC (2013) The European Union summary report on trends and sources of zoonoses, zoonotic agents and food-borne outbreaks in 2011. *J. Eur. Food Safety Auth.* **11**, 3129

4 Anghel, I.B. and Cracium, C. (2013) Self-medication with over-the-counter drugs and antibiotics in Romanian consumers: a qualitative study. *Cogn. Brain Behav.* **17**, 215–235

5 Park, H.J., Kim, J.Y., Kim, J., Lee, J.H., Hahn, J.S., Gu, M.B. et al. (2009) Silver-ion-mediated reactive oxygen species generation affecting bactericidal activity. *Water Res.* **43**, 1027–1032, https://doi.org/10.1016/j.watres.2008.12.002

6 Tran, N., Mir, A., Mallik, D., Sinha, A., Nayar, S. and Webster, T.J. (2010) Bactericidal effects of iron oxide nanoparticles on Staphylococcus aureus. *Int. J. Nanomedicine* **5**, 277–283

7 Berton, V., Montesi, F., Losasso, C., Facco, D.R., Toffan, A. and Terregino, C. (2015) Study of the interaction between silver nanoparticles and Salmonella as revealed by transmission electron microscopy. *J. Prob. Health* **03**, 123

8 Hill, E.K. and Li, J. (2017) Current and future prospects for nanotechnology in animal production. *J. Anim. Sci. Biotechnol.* **8**, 1–13, https://doi.org/10.1186/s40104-017-0157-5

9 Marin, S., Vlasceanu, G., Tiplea, R., Bucur, I., Lemnaru, M. et al. (2015) Applications and toxicity of silver nanoparticles: a recent review. *Curr. Top. Med. Chem.* **15**, 1596–1604, https://doi.org/10.2174/1568026615666150414142209

10 Siddiqi, K.S., Husen, A. and Rao, R.A.K. (2018) A review on biosynthesis of silver nanoparticles and their biocidal properties. *J. Nanobiotechnol.* **16**, 1–28, https://doi.org/10.1186/s12951-018-0334-5

11 de Lima, R., Seabra, A.B. and Durán, N. (2012) Silver nanoparticles: a brief review of cytotoxicity and genotoxicity of chemically and biogenically synthesized nanoparticles. *J. Appl. Toxicol.* **32**, 867–879, https://doi.org/10.1002/jat.2780

12 Ishihara, M., Nguyen, V.Q., Mori, Y., Nakamura, S. and Hattori, H. (2015) Adsorption of silver nanoparticles onto different surface structures of chitin/chitosan and correlations with antimicrobial activities. *Int. J. Mol. Sci.* **16**, 13973–13988, https://doi.org/10.3390/ijms160613973

13 Li, C.W., Wang, Q., Li, J., Hu, M., Shi, S.J., Li, Z.W. et al. (2016) Silver nanoparticles/chitosan oligosaccharide/ poly (vinyl alcohol) nanofiber promotes wound healing by activating TGFbeta1/Smad signaling pathway. *Int. J. Nanomedicine* **11**, 373–386

14 Wang, L.S., Wang, C.Y., Yang, C.H., Hsieh, C.L., Chen, S.Y., Shen, C.Y. et al. (2015) Synthesis and anti-fungal effect of silver nanoparticles-chitosan composite particles. *Int. J. Nanomedicine* **10**, 2685–2696

15 Liu, Y., He, L., Mustapha, A., Li, H., Hu, Z.Q. and Lin, M. (2009) Antibacterial activities of zinc oxide nanoparticles against *Escherichia coli* O157:H7. *J. Appl. Microbiol.* **107**, 1193–1201, https://doi.org/10.1111/j.1365-2672.2009.04303.x

16 Xie, Y.P., He, Y.P., Irwin, P.L., Jin, T. and Shi, X. (2011) Antibacterial activity and mechanism of action of Zinc Oxide nanoparticles against Campylobacter jejuni. *Appl. Environ. Microbiol.* **77**, 2325–2331, https://doi.org/10.1128/AEM.02149-10

17 Kabir, S.M. (2010) Avian colibacillosis and salmonellosis: a closer look at epidemiology, pathogenesis, diagnosis, control and public health concerns. *Int. J. Environ. Res. Public Health* **7**, 89–114, https://doi.org/10.3390/ijerph7010089

18 Khelfa, D.G. and Morsy, E.A. (2015) Incidence and Distribution of some Aerobic Bacterial Agents Associated with High Chick Mortality in some Broiler Flocks in Egypt. *Middle East J. Appl. Sci.* **5**, 383–394, ISSN 2077-4613

19 Hassanen, E.I., Tohamy, A.F., Hassan, A.M., Ibrahim, M.A., Issa, M.Y. and Farroh, K.Y. (2019b) Pomegranate juice diminishes the mitochondrial-dependent cell death and NF-B signaling pathway induced by Copper oxide nanoparticles on the liver and kidneys of rats. *Int. J. Nanomedicine* **14**, 8905–8922, https://doi.org/10.2147/IJN.S229461

20 Hassanen, E.I. and Mohammed, E.R. (2020) In-vivo and In-vitro assessments of the antibacterial potential of chitosan-silver nanocomposite against Methicillin-resistant *Staphylococcus aureus* induced infection in rats. *Biol. Trace Elem. Res.*

21 Hassanen, E.I., Khalaf, A.A., Tohamy, A.F., Mohammed, E.R. and Farroh, K.Y. (2019a) Toxicopathological and immunological studies on different concentrations of chitosan-coated silver nanoparticles in rats. *Int. J. Nanomedicine* **14**, 4723, https://doi.org/10.2147/IJN.S207644

22 Weil, C. (1952) Tables for convenient calculation of median-effective dose (ld50 or ed50) and instructions in their use. *Biometrics* **8**, 249–263, https://doi.org/10.2307/3001557

23 Awaad, M.H., Zoulfakar, S.A., Elhalawaney, M.S., Morsy, E.A., Mohammed, F.F. and El-Refay, R.M. (2019) The impact of sodium-butyrate microencapsulated in balm fat in impedance of colisepticaemia in broiler chickens. *IOSR J. Agric. Vet. Sci.* **12**, 58–69

24 Julian, T.R., Aminul Islam, M., Pickering, A.J., Roy, S., Fuhrmeister, E.R. and Ercumen, A. (2015) Genotypic and phenotypic characterization of *Escherichia coli* isolates from feces, hands, and soils in rural Bangladesh via the Colilert Quanti-Tray System. *Appl. Environ. Microbiol.* **81**, 1735–1743, https://doi.org/10.1128/AEM.03214-14

25 Blanco, J., Blanco, M., Alonso, M.P., Blanco, J.E., Garabal, J. and González, E.A. (1992) Serogroups of *Escherichia coli* strains producing cytotoxic necrotizing factors CNF1 and CNF2. *FEMS Microbiol. Lett.* **96**, 155–159, https://doi.org/10.1111/j.1574-6968.1992.tb05409.x

26 Bancroft, J.D. and Gamble, M. (2002) *Theory and Practice of Histological Techniques, 172-5*, 5th , pp. 593–620, Churchill Living Stone Pub., Edinburgh

27 Hassanen, E.I., Morsy, E.M., Hussien, A.M., Ibrahim, M.A. and Farroh, K.Y. (2020) The effect of different concentrations of gold nanoparticles on growth performance, toxicopathological and immunological parameters of broiler chickens. *Biosci. Rep.* **40**, BSR20194296, https://doi.org/10.1042/BSR20194296

28 Hassanen, E.I., Korany, R.M.S. and Bakeer, A.M. (2021) Cisplatin conjugated gold nanoparticles-based drug delivery system for targeting hepatic tumors. *J. Biochem. Mol. Toxicol.*, Epub ahead of print, https://doi.org/10.1002/jbt.22722

29 Chen, W.Y., Lin, J.Y., Chen, W.J., Luo, L., Wei-Guang Diau, E. and Chen, Y.C. (2010) Functional gold nanoclusters as antimicrobial agents for antibiotic-resistant bacteria. *Nanomedicine* **5**, 755–764, https://doi.org/10.2217/nnm.10.43

30 Grace, A.N. and Pandian, K. (2007) Antibacterial efficacy of aminoglycosidic antibiotics protected gold nanoparticles: a brief study. *Colloids Surf. A Physicochem. Eng. Asp.* **297**, 63–70, https://doi.org/10.1016/j.colsurfa.2006.10.024

31 Rosa, G., Alba, D.F., Silva, A.D., Gris, A., Mendes, R.E. and Mostardeiro, V.B. (2020) Impact of *Escherichia coli* infection in broiler breeder chicks: the effect of oxidative stress on weight gain. *Microb. Pathog.* **139**, 103861, https://doi.org/10.1016/j.micpath.2019.103861

32 Sawah, A.A., Dahshan, H.M., El-Nahass, S. and Abd El-Mawgoud, A.I. (2018) Pathogenicity of *Escherichia coli* O157 in commercial broiler chickens. *J. Basic Appl. Sci.* **7**, 620–625

33 Sharma, V., Jakhar, K.K. and Dahiya, S. (2016) Immuno-pathological studies on broiler chicken experimentally infected with *Escherichia coli* and supplemented with neem (*Azadirachta indica*) leaf extract. *Vet. World* **9**, 735–741, https://doi.org/10.14202/vetworld.2016.735-741

34 Al-Jassani, M.J. and Raheem, H.Q. (2017) Anti-bacterial activity of CuO nanoparticles against some pathogenic bacteria. *Int. J. Chem. Tech. Res.* **10**, 818–822

35 Agarwala, M., Choudhury, B. and Yadav, R.N.S. (2014) Comparative study of antibiofilm activity of copper oxide and iron oxide nanoparticles against multidrug resistant biofilm forming uropathogens. *Indian J. Microbiol.* **54**, 365–368, https://doi.org/10.1007/s12088-014-0462-z

36 Hassanen, E.I., Ibrahim, M.A., Hassan, A.M. et al. (2021) Neuropathological and cognitive effects induced by CuO-NPs in rats and trials for prevention using pomegranate juice. *Neurochem. Res.*, https://doi.org/10.1007/s11064-021-03264-7

37 Morsy, E.A., Hussien, A.M., Ibrahim, M.A., Farroh, K.Y. and Hassanen, E.I. (2021) Cytotoxicity and genotoxicity of copper oxide nanoparticles in chickens. *Biol. Trace Elem. Res.*, https://doi.org/10.1007/s12011-021-02595-4

38 Singh, M., Singh, S., Prasad, S. and Gambhir, I.S. (2008) Nanotechnology in medicine and antibacterial effect of silver nanoparticles. *Dig. J. Nanomater. Biostruct.* **3**, 115–122

39 Hill, E.K. and Li, J. (2017) Current and future prospects for nanotechnology in animal production. *J. Anim. Sci. Biotechnol.* **8**, 26, https://doi.org/10.1186/s40104-017-0157-5

40 Pineda, L., Chwalibog, A., Sawosz, E., Lauridsen, C., Engberg, R., Elnif, J. et al. (2012) Effect of silver nanoparticles on growth performance, metabolism and microbial profile of broiler chickens. *Arch. Anim. Nutr.* **66**, 416–429, https://doi.org/10.1080/1745039X.2012.710081

41 Badawy, M.E., Lotfy, T.M. and Shawir, S.M. (2019) Preparation and antibacterial activity of chitosan-silver nanoparticles for application in preservation of minced meat. *Bull. Natl. Res. Cent.* **43**, 83, https://doi.org/10.1186/s42269-019-0124-8

42 Maillard, J. and Hartemann, P. (2012) Silver as an antimicrobial: facts and gaps in knowledge. *Crit. Rev. Microbiol.* **39**, 373–383, https://doi.org/10.3109/1040841X.2012.713323

43 Radu, F., Rotariu, L. and Butnariu, M. (2018) Inactivation of St. Aureus and Escherichia coli by essential oil from sage (salvia species) in telemea cheese. *International Multidisciplinary Scientific GeoConference Surveying Geology and Mining Ecology Management, SGEM* **18**, 187–194, https://doi.org/10.5593/sgem2018V/6.4/S08.024

44 Farouk, M.M., El-Molla, A., Salib, F.A., Soliman, Y.A. and Shaalan, M. (2020) The role of silver nanoparticles in a treatment approach for multidrug-resistant Salmonella species isolates. *Int. J. Nanomedicine* **15**, 6993–7011, https://doi.org/10.2147/IJN.S270204

45 Negrea, P., Caunii, A., Sarac, I. and Butnariu, M. (2015) The study of infrared spectrum of chitin and chitosan extract as potential sources of biomass. *Digest J. Nanomater. Biostruct.* **10**, 1129–1138

46 Chen, C.W., Hsu, C.Y., Lai, S.M., Syu, W.J., Wang, T.Y. and Lai, P.S. (2014) Metal nanobullets for multidrug resistant bacteria and biofilms. *Adv. Drug Deliv. Rev.* **78**, 88–104, https://doi.org/10.1016/j.addr.2014.08.004

47 Du, W., Niu, S., Xu, Y., Xu, Z. and Fan, C. (2009) Antibacterial activity of chitosan tripolyphosphate nanoparticles loaded with various metal ions. *Carbohydr. Polym.* **75**, 385–389, https://doi.org/10.1016/j.carbpol.2008.07.039

48 Vardanian, A., Kurzbaum, E., Farber, Y., Butnariu, M. and Armon, R. (2018) Facilitated enumeration of the silicate bacterium Paenibacillus mucilaginosus comb. nov. (formerly Bacillus mucilaginosus) via tetrazolium chloride incorporation into a double agar-based solid growth medium. *Folia Microbiol. (Praha)* **63**, 401–404, https://doi.org/10.1007/s12223-017-0567-y

49 Huh, A.J. and Kwon, Y.J. (2011) "Nanoantibiotics": a new paradigm for treating infectious diseases using nanomaterials in the antibiotics resistant era. *J. Control. Release* **156**, 128–145, https://doi.org/10.1016/j.jconrel.2011.07.002

50 Shaalan, M., El-Mahdy, M., Theiner, S., Dinhopl, N., El-Matbouli, M. and Saleh, M. (2018) Silver nanoparticles: their role as antibacterial agent against Aeromonas salmonicida subsp. salmonicida in rainbow trout (Oncorhynchus mykiss). *Res. Vet. Sci.* **119**, 196–204, https://doi.org/10.1016/j.rvsc.2018.06.019

51 Fondevila, M. (2010) Potential use of silver nanoparticles as an additive in animal feeding. In *Silver Nanoparticles* (Pozo Perez, D., ed.), Springer
    International Publishing, Houston, TX, U.S.A., ISBN: 978-953-307-028-5 http://www.intechopen.com/books/silver-nanoparticles ,
    https://doi.org/10.5772/8509

52 Wang, B., He, X., Zhang, Z., Zhao, Y. and Feng, W. (2013) Metabolism of nanomaterials in vivo: blood circulation andorgan clearance. *Acc. Chem. Res.*
    46, 761–769, https://doi.org/10.1021/ar2003336

53 Nabinejad, A.R., Noaman, V. and Khayam Nekouei, S.M. (2016) Evaluation of silver residues accumulation in tissues of Broilers treated with nanosilver
    using MNSR (a clinical trial). *Arch. Razi Inst.* **71**, 51–55

54 Kalaivani, R., Maruthupandy, M., Muneeswaran, T., Hameedha Beevi, A., Anand, M., Ramakritinan, C.M. et al. (2018) Synthesis of chitosan mediated
    silver nanoparticles (ag nps) for potential antimicrobial applications. *Front. Lab. Med.* **2**, 30–35, https://doi.org/10.1016/j.flm.2018.04.002

55 Zienkiewicz-Strzalka, M., Derylo-Marczewska, A., Skorik, A.Y., Petrova, V.A., Choma, A. and Komaniecka, I. (2020) Silver nanoparticles on
    chitosan/silica nanofibers: characterization and antibacterial activity. *Int. J. Mol. Sci.* **21**, 166, https://doi.org/10.3390/ijms21010166

56 Krishnaveni, B. and Ragunathan, R. (2015) Extraction and characterization of chitin and chitosan from f.Solani cbnr bkrr, synthesis of their
    bionanocomposites and study of their productive application. *J. Pharm. Sci. Res.* **7**, 197–205